Published in final edited form as:
Cancer Cell. 2010 February 17; 17(2): 121–134. doi:10.1016/j.ccr.2009.12.019.

FcRγ Activation Regulates Inflammation-Associated Squamous Carcinogenesis

Pauline Andreu[1,5], **Magnus Johansson**[1,5], **Nesrine I. Affara**[1,5], **Ferdinando Pucci**[3], **Tingting Tan**[1], **Simon Junankar**[1], **Lidiya Korets**[1], **Julia Lam**[1], **David Tawfik**[1], **David G. DeNardo**[1], **Luigi Naldini**[3], **Karin E. de Visser**[4], **Michele De Palma**[3], and **Lisa M. Coussens**[1,2,*]

[1]Department of Pathology University of California, San Francisco, San Francisco, CA 94143, USA [2]Helen Diller Family Comprehensive Cancer Center University of California, San Francisco, San Francisco, CA 94143, USA [3]Angiogenesis and Tumor Targeting Research Unit, San Raffaele-Telethon Institute for Gene Therapy and Vita-Salute San Raffaele University, San Raffaele Institute, Milan, 20132, Italy [4]Division of Molecular Biology, The Netherlands Cancer Institute, Amsterdam, 1066 CX, the Netherlands

SUMMARY

Chronically activated leukocytes recruited to premalignant tissues functionally contribute to cancer development; however, mechanisms underlying pro- versus anti-tumor programming of neoplastic tissues by immune cells remain obscure. Using the K14-HPV16 mouse model of squamous carcinogenesis, we report that B cells and humoral immunity foster cancer development by activating Fcγ receptors (FcγRs) on resident and recruited myeloid cells. Stromal accumulation of autoantibodies in premalignant skin, through their interaction with activating FcγRs, regulate recruitment, composition, and bioeffector functions of leukocytes in neoplastic tissue, which in turn promote neoplastic progression and subsequent carcinoma development. These findings support a model in which B cells, humoral immunity, and activating FcγRs are required for establishing chronic inflammatory programs that promote de novo carcinogenesis.

INTRODUCTION

Clinical, epidemiological, and experimental studies have established that chronic inflammation contributes to various aspects of solid tumor development (de Visser et al., 2006; Mantovani et al., 2008). In particular, chronic inflammatory diseases, including several autoimmune disorders, are associated with increased risk of cancer development (Brandtzaeg et al., 2006; Dalgleish and O'Byrne, 2002), revealing that B cell hyperactivity combined with altered cellular immunity cooperate to initiate and/or sustain persistent inflammation that enhances overall cancer risk in afflicted tissues.

Deposition of B lymphocyte-derived immunoglobulins (Igs) is a common occurrence in premalignant and malignant stroma of human cancers (de Visser et al., 2006; Tan and Coussens, 2007). In addition, high levels of circulating immune complexes (CIC) are associated with increased tumor burden and poor prognosis in patients with breast,

*Correspondence: lisa.coussens@ucsf.edu.
[5]These authors contributed equally to this work

SUPPLEMENTAL INFORMATION Supplemental Information includes five figures, Supplemental Experimental Procedures, and one table and can be found with this article online at doi:10.1016/j.ccr.2009.12.019.

genitourinary, and head and neck malignancies (Tan and Coussens, 2007). While little is known about the function of CICs in tumor development, the role of CICs in inflammatory and autoimmune diseases is undisputed. CIC deposition in stroma has been implicated as an initiator of inflammatory cascades by mechanisms that include activation of complement pathways and engagement of the receptors for the crystallizable region (Fc) of IgG (FcγRs) on the surface of leukocytes (Takai, 2005). As such, FcγRs represent a functional link between adaptive and innate immunity by coupling interactions between circulating (auto)antibodies and innate immune cells (Nimmerjahn and Ravetch, 2008).

Four classes of IgG receptor FcγRs have been identified, FcγRI/CD64, FcγRII/CD32, FcγRIII/CD16, and FcγRIV, differing by their distinct affinity for IgG isotypes, cellular distributions, and effector functions (Nimmerjahn and Ravetch, 2008). Activating types of FcγRs form multimeric complexes including the Fc receptor common γ chain (FcRγ) that contains an intracellular tyrosine-based activating motif (ITAM), whose activation triggers oxidative bursts, cytokine release, phagocytosis, antibody-dependent cell-mediated cytotoxicity, and degranulation (Takai, 2005). In contrast, engagement of FcγRIIB (or FcγRII in mice), which contains an immune tyrosine-based inhibitory motif, abrogates ITAM-mediated inflammatory responses and instead regulates alternative signaling cascades (Takai, 2005). FcRγ expression is necessary for assembly and cell-surface localization of FcγRI, FcγRIII, and FcγRIV; as such, FcR$\gamma^{-/-}$ mice (Takai et al., 1994) are deficient for all activating FcγRs, whereas FcγRII expression is unaltered. Given that developing solid tumors display similar characteristics to tissues damaged by autoimmune dysfunction, e.g., chronic immune cell infiltration, tissue remodeling, angiogenesis, and altered cell survival pathways, we speculated that similar humoral immune-mediated regulatory pathways may be involved in solid tumor development.

Using a transgenic mouse model of multistage epithelial carcinogenesis, i.e., K14-HPV16 mice (Coussens et al., 1996), we previously revealed that adaptive immunity is an important regulator of inflammation-associated cancer development (de Visser et al., 2005). Combined B and T lymphocyte deficiency in HPV16 mice, e.g., HPV16/RAG1$^{-/-}$ mice, resulted in a failure to initiate and/or sustain leukocyte infiltration during premalignancy (de Visser et al., 2005). As a consequence, tissue remodeling, angiogenesis, and epithelial hyperproliferation were significantly reduced, culminating in attenuated premalignant progression and a 43% reduction in carcinoma incidence (de Visser et al., 2005). Importantly, adoptive transfer of B lymphocytes or serum from HPV16 mice into HPV16/RAG1$^{-/-}$ mice reinstated chronic inflammation in premalignant tissues, indicating that B cell-derived soluble mediators were necessary to potentiate malignant progression. In the present study, we investigated whether B cell-derived IgGs regulate neoplastic progression and subsequent carcinoma development by engagement of FcγRs expressed on resident and recruited immune cells.

RESULTS

Humoral Immunity-Mediated Promotion of Squamous Carcinogenesis in HPV16 Mice

HPV16 mice express the early region genes of human papilloma-virus type 16 (HPV16) under control of the human keratin 14 promotor/enhancer (Arbeit et al., 1994). By 1 month of age, HPV16 mice develop epidermal hyperplasias with 100% penetrance characterized by a terminally differentiated hyperproliferative epidermis. Between 3 and 6 months of age, hyperplastic lesions advance focally into angiogenic dysplasias with prominent hyperproliferative epidermis that fails to undergo terminal differentiation and a dermis containing significant CD45^{+} leukocyte infiltration encompassing CD117^{+} mast cells and CD11b^{+}Gr1^{+} immature myeloid cells (IMCs; Coussens et al., 1999; de Visser et al., 2005; Junankar et al., 2006) (Figures 1A–1H). By 1 year of age, 60% of HPV16 mice (FVB/n, N25) develop malignant skin carcinomas, 50% of which are squamous cell carcinomas

(SCCs) that metastasize to regional lymph nodes with a ~30% frequency (Coussens et al., 1996). HPV16 mice lacking mast cells (Coussens et al., 1999), leukocyte-derived matrix metalloproteinase (MMP)-9 (Coussens et al., 2000), or B and T lymphocytes, e.g., HPV16/RAG1$^{-/-}$ mice (de Visser et al., 2005), exhibit attenuated parameters of premalignant progression culminating in reduced SCC development.

Given that adoptive transfer of B cells or serum (isolated from HPV16 mice) into HPV16/RAG1$^{-/-}$ mice restored hallmarks of premalignant progression (de Visser et al., 2005), we hypothesized that humoral immunity represented the critical feature of premalignant progression regulating chronic inflammation. To investigate this, we generated HPV16 mice deficient for B220^{+}CD19^{+} mature B cells (Chen et al., 1993), e.g., HPV16/JH$^{-/-}$ mice (Figure S1A, available online). Similar to HPV16/RAG1$^{-/-}$ mice, HPV16/JH$^{-/-}$ mice exhibited reduced infiltration of premalignant skin by CD45^{+} leukocytes, including mast cells and Gr1^{+} myeloid cells (Figures 1A–1C). Whereas CD11b^{+}Gr1^{+}F4/80^{-}CD11c^{-} IMCs constitute the most abundant CD45^{+} leukocyte subtype in premalignant HPV16 skin (Figures 1D and 1E), immune cell infiltrates in HPV16/JH$^{-/-}$ mice instead revealed an increased relative proportion of CD11b^{+}Gr1^{-} cells (Figure 1D) that contained F4/80^{+} and CD11c^{+} cells (Figure 1E), as well as expanded populations of CD3^{+}CD4^{+} and CD3^{+}CD8^{+} T cells (Figure 1D). In addition, HPV16/JH$^{-/-}$ mice exhibited reduced presence of CD31^{+} blood vessels (Figure 1F), vascular endothelial growth factor (VEGF), and MMP-9 protein levels (Figure 1G and Figure S1B); reduced keratinocyte hyperproliferation (Figure 1H); and diminished presence of focal dysplastic lesions (Figure 1I). Together, these data indicate that B cells are critical components of adaptive immunity regulating premalignant progression and characteristics of early squamous carcinogenesis in HPV16 mice.

HPV16-Induced Autoantibody Complexes Induce Acute Inflammation

Because parameters of premalignant progression were reinstated in HPV16/RAG1$^{-/-}$ mice by adoptive transfer of serum from HPV16 animals, and because dysplastic skin of HPV16 mice is characterized by stromal depositions of IgG and IgM (de Visser et al., 2005), we hypothesized that Igs were the mediators by which B cells promote premalignant progression. To assess this, we first evaluated CIC presence in serum of HPV16 mice and found increased concentrations paralleling premalignant progression (Figure 2A). Using direct immunofluorescence with biotinylated IgGs isolated from HPV16 serum (IgG_{HPV16}) as detector antibodies, we revealed that IgG_{HPV16} cognate antigens were localized to both epithelial and dermal compartments of neoplastic skin (Figure 2B, inset). In addition to HPV16 E7 oncoprotein-specific autoantibodies (Figure S2) (Daniel et al., 2005), we identified high titer IgGs specific for type I, II, and IV collagens, but not laminins 111 and 332 (Figure 2B).

To determine whether stromal deposition of autoantibodies was sufficient to induce an acute inflammatory response in vivo, we injected IgG_{HPV16} versus IgG isolated from negative littermate mice (IgG_{wt}) intradermally into syngeneic FVB/n mice. While IgG_{HPV16} and IgG_{wt} antibodies were similarly detected in dermis (Figure 2C), only mice injected with IgG_{HPV16} exhibited an acute inflammatory response characterized by a significant increase in CD45^{+} and Gr1^{+} cell recruitment (Figure 2D). Since similar concentrations of IgG_{HPV16} versus IgG_{wt} differentially induced leukocyte recruitment in vivo, we hypothesized that higher proportions of IgG_{HPV16} as opposed to IgG_{wt} were present in their active form, e.g., in immune complexes (ICs), and indeed, we found that IgG_{HPV16} contains significantly higher levels of both IgG/C3 and IgG/C1q ICs as compared to IgG_{wt} (Figure 2E).

Differential Expression of FcγR Ig Receptors on Leukocytes in HPV16 Neoplastic Skin

Premalignant progression in HPV16 mice is independent of complement cascade activation via complement factor C3 (de Visser et al., 2004); thus, we hypothesized that CICs accumulating in young HPV16 mice promoted neoplastic progression through activation of FcRγ signaling. FcγRs are broadly expressed on immune cells and encompass both activating, e.g., FcγRI, III, and IV (including the FcRγ subunit), and inhibitory, e.g., FcγRII, subtype complexes (Nimmerjahn and Ravetch, 2008). Immunodetection of FcRγ, FcγRI, and FcγRII/III revealed increased presence of $CD45^+Fc\gamma R^+$ cells in dermal regions of premalignant HPV16 skin (Figure 3A). Using flow cytometry, we revealed that while $CD11b^+Gr1^+$ IMCs and $CD45^+CD117^+$ mast cells expressed FcγRIII, $CD11b^+Gr1^-$ cells, including $F4/80^+$ macrophages and $CD11c^+$ dendritic cells (DCs), expressed FcγRI and FcγRIII, and no expression of any FcγR was detected on $CD3^+$ T cells or $CD45^-$ nonimmune cells in neoplastic skin (Figure 3B). B cells were not evaluated given their undetectable levels in HPV16 skin (Figure 1D) (de Visser et al., 2005).

Leukocyte FcRγ Is Necessary for Tumor Development and Squamous Carcinogenesis

Because IgG_{HPV16} induced acute inflammatory responses in syngeneic nontransgenic mice, and proinflammatory-type FcγRs were expressed on infiltrating leukocytes in premalignant HPV16 skin, we evaluated whether carcinoma growth or de novo squamous carcinogenesis were FcγR dependent. First we assessed transplantable tumor growth with syngeneic $FcR\gamma^{-/-}$ (Takai et al., 1994) versus $FcR\gamma^{+/-}$ mice injected subcutaneously with PDSC5 cells, a carcinoma cell line derived from a poorly differentiated SCC (Arbeit et al., 1996). Mice lacking FcRγ failed to mount a robust angiogenic response (Figure 3C) as well as to support transplantable tumor growth (Figure 3D), which was independent of humoral immune responsiveness as serum Ig titers increased in PDSC5-injected mice irrespective of FcRγ expression (Figure 3D).

To evaluate whether de novo tumorigenesis was similarly FcRγ dependent, we generated a cohort of HPV16/$FcR\gamma^{-/-}$ mice that retained expression of inhibitory FcγRII (Figure S3A). Quantitative evaluation of $CD45^+$ immune cell infiltrates in neoplastic skin by flow cytometry revealed reduced leukocyte infiltration in HPV16/$FcR\gamma^{-/-}$ mice as compared to age-matched HPV16/$FcR\gamma^{+/-}$ tissue (Figure 4A). Similar to HPV16/$JH^{-/-}$ mice, mast cells and IMCs were significantly reduced in HPV16/$FcR\gamma^{-/-}$ mice, concomitant with an increased relative influx of $CD11b^+Gr1^-$ macrophages and DCs, as well as $CD3^+CD4^+$ and $CD3^+CD8^+$ lymphocytes (Figures 4B–4D). F4/80 and CD11c lineage marker expression on both $CD11b^+Gr1^+$ and $CD11b^+Gr1^-$ cells were unperturbed by absence of FcRγ (Figure 4E and Figure S3D). FcγRIII-expressing $CD45^+CD49b^+CD3^-$ NK cells represented a minor population in control HPV16 skin, recruitment of which was not modified by FcRγ deficiency (Figures S3B and S3C).

To determine whether the activating types of FcγRs also mediated other parameters of de novo squamous carcinogenesis, we analyzed age-matched HPV16/$FcR\gamma^{-/-}$ mice at canonical time points (1, 4, and 6 months of age) and found reduced development of angiogenic vasculature (Figure 4F), VEGF, and MMP-9 protein levels (Figure 4G and Figure S3E); reduced keratinocyte hyperproliferation and appearance of focal dysplastic regions (Figures 4H and 4I); and significantly reduced incidence of SCC development (Figure 4I). Diminished de novo carcinogenesis in HPV16/$FcR\gamma^{-/-}$ mice was independent of B cell responses and humoral immunity as shown by Ig isotype switching and accumulation of IgG_1 and IgG_{2a} in HPV16/$FcR\gamma^{-/-}$ mice (Figure S3F). Our interpretation of these findings was that peripheral activation of humoral immunity in young HPV16 mice promoted squamous carcinogenesis by locally activating FcRγ-mediated signaling on resident and recruited immune cells in neoplastic skin. These in turn activate angiogenic

programs in vascular cells, thus enabling tissue expansion via keratinocyte hyperproliferation, culminating in increased SCC development.

Mast Cell FcRγ Activation Regulates Parameters of Premalignant Progression and Enhances Tumor Development

Given that we found that combinations of activating FcγRs were expressed on infiltrating leukocytes in HPV16 skin, and given that absence of either humoral immunity or FcRγ altered leukocyte composition during premalignant composition, we sought to delineate which distinct FcRγ$^+$ leukocyte population exhibited protumorigenic properties.

FcγRIII$^+$ mast cells regulate tissue remodeling, angiogenesis, and keratinocyte hyperproliferation in HPV16 mice (Coussens et al., 1999; Coussens et al., 2000), thus we evaluated whether FcRγ-dependent activation of mast cells was in part necessary for neoplastic progression. Using conditioned medium generated from FcRγ-deficient versus FcRγ-proficient bone marrow-derived mast cells (BMMCs) previously stimulated with either rat IgG, IgG_{HPV16}, or IgG_{wt}, we found that Ig-activated mast cells induced human umbilical vein endothelial cell (HUVEC) migration (Figure 5A), VEGF expression (Figure 5B), and CD45$^+$ peripheral blood leukocyte (PBL) recruitment (Figure 5C), which were dependent on FcRγ expression. The diminished capabilities of FcRγ-deficient mast cells were conserved in vivo as PDSC5 tumor growth was significantly diminished in mast cell-deficient (kit$^{sh/sh}$) mice, whereas presence of FcRγ-proficient BMMCs significantly enhanced tumor growth, development of angiogenic vasculature, and infiltration by Gr1$^+$ leukocytes (Figures 5D and 5E). These features were not significantly altered in PDSC5 tumors grown in the presence of FcRγ$^{-/-}$ BMMCs as compared to PDSC5 cells alone (Figure 5E). Thus, these findings support a model in which mast cells respond to CIC deposition in early neoplastic stroma by activating FcγR-mediated pathways, leading to PBL recruitment and angiogenesis, which together establish a microenvironment permissive for tumor development.

FcRγ-Independent and -Dependent Properties of CD11b$^+$ Myeloid Cells in HPV16 Mice

As described both in cancer patients and mice harboring some transplantable tumors (Ostrand-Rosenberg, 2008), CD11b$^+$Gr1$^+$ cells accumulate in spleen and peripheral blood of HPV16 mice (Figure S4A). Morphological analysis of CD11b$^+$Gr1$^+$ cells isolated from neoplastic skin and spleen of HPV16 mice revealed characteristics of immature granulocytes, including presence of elongated band-shaped, nonfragmented nuclei (Figure 6A) in cells encompassing a mixed population expressing CD45, 7/4, CD14, CD44, IL4Rα, CD80, and CD86, but not CD34 (Figure S4B). In contrast, CD11b$^+$Gr1$^-$ cells (from skin) accumulate only in draining lymph nodes of HPV16 mice (Figure S4A), exhibited a more mature phenotype with larger cellular diameters, dense granules, vacuole-rich cytoplasm, and round nuclei (Figure 6A), and reflected subpopulations orientated toward dendritic (CD11c$^+$) and macrophage lineages (F4/80$^+$) (Figure S4B).

To delineate which distinct FcRγ$^+$ myeloid population present in HPV16 neoplastic skin exerted FcRγ-dependent protumor properties, and considering the fact that differential activation of FcγRs regulates DC maturation (Takai, 2005), we evaluated expression of CD86, CD80, and MHC-II by flow cytometry in CD11b$^+$Gr1$^-$CD11c$^+$F4/80$^-$ DCs from cervical lymph nodes and premalignant skin of HPV16/FcRγ$^{+/-}$ and HPV16/FcRγ$^{-/-}$ mice and found no significant differences (Figure S5A). Similarly, when we audited gene expression of CD11b$^+$Gr1$^-$CD11c$^+$F4/80$^-$ skin DCs isolated from age-matched HPV16/FcRγ$^{+/-}$ and HPV16/FcRγ$^{-/-}$ mice by low-density qPCR arrays, we found no change in expression of genes reflecting DC maturation. However, HPV16/FcRγ$^{-/-}$ DCs reflected

myeloid population polarized toward a T_H1 state as shown by enhanced expression of *Nos2*, *IL1a*, *IFN*g, *IL12a*, *Ptgs2*, and *IL6* (Figure S5B and Table S1).

$CD11b^+Gr1^+$ myeloid-derived suppressor cells (MDSCs) have been reported to promote tumor development by enhancing angiogenesis and by inhibiting T lymphocyte-mediated anti-tumor immunity (Ostrand-Rosenberg, 2008). Since $CD11b^+Gr1^+$ accumulate in HPV16 neoplastic tissue and peripheral sites and exhibit an immature morphology (Figure 6A and Figure S4B), we assessed their immune-suppressive capabilities as compared to $CD11b^+Gr1^+$ cells isolated from tumors and spleens of 4T1 mammary tumor-bearing mice, a model where immune-suppressive properties of MDSCs have been previously described (Figure S5C) (Ostrand-Rosenberg, 2008). Neither $CD11b^+Gr1^+$ cells isolated from premalignant skin nor from spleen of HPV16 mice demonstrated in vitro inhibition of polyclonal activation of either $CD4^+$ or $CD8^+$ T cells (Figure S5C). In addition, $CD11b^+Gr1^+$ cells failed to produce reactive oxygen species, major mediators implicated in myeloid-mediated immune suppression (Figure S5D) (Ostrand-Rosenberg, 2008). Moreover, using low-density qPCR arrays, gene expression analysis of HPV16/FcR$\gamma^{-/-}$ versus HPV16/FcR$\gamma^{+/-}$ skin $CD11b^+Gr1^+$ cells revealed downregulation of *IL1a*, *Ptgs2*, and *TNFα*, indicative of a diminished proinflammatory state (Figure S5E and Table S1). Moreover, when co-injected with PDSC5, $CD11b^+Gr1^+$ cells isolated from skin of HPV16 mice failed to alter either tumor growth or development of angiogenic vessels (Figures 6B and 6C) and did not exhibit proangiogenic activity in vitro (Figure 6D). Thus, although present in significant numbers, $CD11b^+Gr1^+$ cells infiltrating neoplastic skin are likely to represent a population of bona fide immature cells.

FcRγ Activation Mediates the Protumor and Angiogenic Bioactivities of $CD11b^+Gr1^-F4/80^+$ Macrophages

In contrast to IMCs, both spleenic and skin $CD11b^+Gr1^-CD11c^-F4/80^+$ macrophages induced HUVEC migration in vitro by a FcRγ-dependent mechanism (Figure 6D) and significantly enhanced PDSC5 tumor growth in vivo (Figures 6B and 6C). Moreover, macrophage-enhanced tumorgenicity of PDSC5 cells was also FcRγ dependent (Figures 7A and 7B). Interestingly, bone marrow-derived FcR$\gamma^{-/-}$ macrophages, when admixed with PDSC5 cells, not only failed to promote transplantable tumor development but also impeded tumor growth (Figure 7B).

Given that DC gene expression analyses revealed altered programming toward a T_H1-type state, we reasoned that perhaps, similarly, in the absence of FcRγ signaling, macrophages were also reprogrammed. Indeed, using low-density qPCR arrays and RT-PCR, gene expression analyses of macrophages isolated from HPV16/FcR$\gamma^{+/-}$ versus HPV16/FcR$\gamma^{-/-}$ skin revealed significant upregulation of genes reflecting classical “M1” activation, including *Il1b*, *Il12a*, *Cxcl10*, *Nos2*, *Cxcl11*, and *IL1a*, whereas genes reflecting alternative “M2” (*Il13*, *Cd163*, *Ccl17*, *Il4*, and *Ym1*) or “M2-like” (*Ccl1*) activation were significantly downregulated in HPV16/FcR$\gamma^{-/-}$ as compared to HPV16/FcR$\gamma^{+/-}$ macrophages (Figure 7C).

Among the differentially expressed genes, the angiostatic chemokines *Cxcl10 and Cxcl11* were significantly elevated in HPV16/FcR$\gamma^{-/-}$ macrophages (Figure 7C). We confirmed that mRNA expression of *Cxcl10*, as well as its receptor *Cxcr3*, were significantly upregulated in whole neoplastic skin of 4-month-old HPV16/FcR$\gamma^{-/-}$ and HPV16/JH$^{-/-}$, as compared to age-matched HPV16/FcR$\gamma^{+/-}$ skin by qRT-PCR (Figure 7D). Given that VEGF-induced HUVEC migration was significantly inhibited by CXCL10 in a CXCR3-dependent manner (Figure 7E), we evaluated FcRγ-deficient versus FcRγ-proficient macrophages isolated from the respective HPV16 cohorts and revealed CXCR3-dependent angiostatic activity of FcR$\gamma^{-/-}$ macrophages (Figure 7F).

DISCUSSION

We revealed a provocative and functional role for B cells and activating type FcγRs as potentiators of squamous carcinogenesis. Using a transgenic mouse model of epithelial carcinogenesis and mice lacking either B cells or activating FcγRs, we found that IC stimulation of leukocyte FcRγ is critical for establishing a protumor microenvironment in premalignant tissue that directs not only recruitment of leukocytes from peripheral blood but also leukocyte composition, phenotype, and bioeffector functions once within neoplastic tissue (Figure 8). As such, proangiogenic and protumorigenic functions of mast cells and macrophages are differentially regulated by humoral immunity and functionally contribute to squamous carcinogenesis (Figure 8). These findings have broad clinical implications as they reveal critical signaling pathways regulated by humoral immunity and FcRγ to target therapeutically in patients at risk for cancer development, e.g., patients suffering from chronic inflammatory diseases, as well as individuals harboring premalignant lesions where chronic inflammation compromises tissue integrity and enhances risk of malignancy.

Regulation of Protumor Immunity by B Cells, Humoral Immunity, and Activating FcγRs

While early and persistent inflammatory-type reactions in or around developing neoplasms are thought to regulate tumor development (de Visser et al., 2005; Mantovani et al., 2008), tumor-promoting properties of adaptive leukocytes have not been fully elucidated. As the central component of humoral immunity, B lymphocytes function in antibody production, antigen presentation, and secretion of proinflammatory cytokines. In the context of cancer, in addition to altering local and circulating levels of cytokines, B cells also inhibit T_H1-mediated anti-tumor immunity. In a transplantable model of colorectal cancer, partial B cell depletion resulted in significantly reduced tumor burden (Barbera-Guillem et al., 2000), while B cell-deficient mice showed resistance to syngeneic tumors (Shah et al., 2005). In addition, overexpression of tumor necrosis factor receptor-associated factor 3 in lymphocytes activates humoral immune responses that result in chronic inflammation and enhanced incidence of cancer, particularly SCCs (Zapata et al., 2009).

Using HPV16/B cell-deficient mice, we found that pre-malignant progression was significantly attenuated and essentially stalled at an early hyperplastic stage. In the absence of B cells, leukocyte recruitment from peripheral blood was reduced, vasculature failed to mount an angiogenic response, and hyperproliferation of keratinocytes failed to support tissue expansion to a carcinoma in situ state. Thus, peripheral activation of B cells represents an early event in premalignant progression that promotes subsequent neoplastic programming of tissue.

How do B cells “promote” solid tumor formation? It is well known that cancer patients develop antibodies to tumor-associated antigens—evidence exist for c-*myc*, HER-2/neu, and p53 (Lu et al., 2008). In addition, high circulating levels of ICs are associated with increased tumor burden and poor prognosis in patients with breast, genitourinary, and head and neck malignancies (Tan and Coussens, 2007). In a chemical carcinogenesis mouse model of papilloma growth, immunization against an inherited oncoprotein failed to eradicate tumor cells but rather induced tumor growth (Siegel et al., 2000). Increased levels of Ig in neoplastic microenvironments result in accumulation of ICs that favor tumor-promoting inflammatory responses including recruitment and activation of several myeloid cell types (Barbera-Guillem et al., 1999). When injected into syngeneic nontransgenic mice, CICs (from HPV16 mice) alone were sufficient to trigger an acute inflammatory response. While largely not described in the context of cancer, the significance of inflammatory responses to autoantibodies has been studied in mouse models of autoimmune disease (Nimmerjahn and Ravetch, 2008) where FcγRs have been recognized as effectors that induce recruitment of CD11b-expressing myeloid cells into tissue (Bergtold et al., 2006). Thus, mice deficient in

activating-type FcγRs are resistant to IC-mediated hypersensitive reactions, such as alveolitis, glomerulonephritis, and skin Arthus reaction, while mice deficient in FcγRII exhibit enhanced IC-mediated inflammatory responses (Takai, 2005). Herein, we found differential presence of both activating and inhibitory types of FcγRs on infiltrating myeloid cells, and using FcRγ-deficient mice, we demonstrated a functional role for the Fc activating receptors in cancer promotion. Therefore IgG-mediated activation of FcRγ on resident and recruited leukocytes, including mast cells and macrophages, regulated not only PBL recruitment but also leukocyte activation and bioeffector function within the neoplastic microenvironment.

Activation of complement pathways is an alternative mechanism by which IgG could induce leukocyte activation and recruitment, further leading to chronic inflammation. Markiewski et al. (2008) reported that transplanted renal tumor growth was regulated by complement activation and that C5a deposition was associated with MDSC recruitment and subsequent CTL suppression. Complement factor C3 does not alter parameters of neoplastic progression in HPV16 mice (de Visser et al., 2005); however, C3-independent mechanisms do exist (Baumann et al., 2001). As such, we cannot exclude a role for complement factors as sensors of IC deposition in HPV16 mice, potentially regulating C3-independent FcγR activation.

It is intriguing to speculate that targeting B lymphocyte/Ig/FcγR pathway by inactivating either B lymphocytes or FcRγ signaling may be tractable for anti-cancer therapy. In support of this approach, patients with rheumatoid arthritis, systemic lupus erythematosus, and others, have benefited following B cell-depletion therapy using a chimeric monoclonal antibody specific to human CD20, e.g., Rituximab (Gurcan et al., 2009). Rituximab has also shown clinical efficacy in adult acute lymphoblastic leukemia (Gokbuget and Hoelzer, 2006). Support for extending Rituximab into solid tumor therapy comes from a clinical study with colon cancer patients in which numbers of CD21-hyperpositive lymphocytes were reduced in parallel with reduction in tumor burden (Barbera-Guillem et al., 2000). Although Rituximab effectively deletes circulating B cells, no increased susceptibility to infection has been observed in patients with rheumatoid arthritis or non-Hodgkin's lymphoma (Gokbuget and Hoelzer, 2006), thus supporting the approach and manipulation of humoral immunity and/or its downstream effector pathways as a therapeutic possibility.

Programming Recruited Leukocytes and Inhibiting Protumor Immunity

Clinical and experimental data indicate that chronic presence and activation of immune cells, e.g., mast cells, macrophages, Tie2-expressing monocytes, neutrophils, DCs, IMCs, and $CD4^+$ T cells, promote tumor development by activating angiogenic programs, suppressing antitumor immunity (Mantovani et al., 2008), and enhancing tumor cell migration and metastasis (DeNardo et al., 2009; Pollard, 2008). When chronically activated in tumor microenvironments, some myeloid cells are programmed such that they deliver a diversity of bioactive mediators to neoplastic tissues, including chemokines, cytokines, matrix remodeling enzymes, and cytotoxic proteins (Mantovani et al., 2008). Identification of the critical programs that induce these protumor pathways would reveal important mediators to potentially target with anticancer therapeutics.

Mast cells exert duality as cancer mediators with some clinical studies indicating their presence in human cancers correlates with a favorable clinical outcome, whereas others clearly implicate them as protumor mediators (Theoharides and Conti, 2004). In HPV16 mice (Coussens et al., 1999), and in other models of cancer development (Nakayama et al., 2004; Soucek et al., 2007), mast cell-derived factors foster tumor cell survival and angiogenesis. With IgG-mediated stimulation of mast cells enhancing tumor development and angiogenesis in HPV16 mice, these data indicate a functional requirement for FcRγ

engagement for activating protumor cascades, leading to PBL recruitment into neoplastic skin, angiogenesis, and tumor development.

Pharmacologic inhibition of macrophages minimizes cervical carcinogenesis in HPV16 mice (Giraudo et al., 2004), whereas elimination of macrophages during mammary carcinogenesis limits cancer progression and metastasis (Pollard, 2008) by reducing angiogenesis in premalignant tissues. Interestingly, pro- versus anti-metastatic properties of infiltrating macrophages in MMTV-PyMT mice are programmed by $CD4^+$ T lymphocytes via an IL-4-dependent mechanism (DeNardo et al., 2009). In contrast, in ovarian cancer, macrophage pheno-type is regulated by IL-1R and MyD88, which together maintain a macrophage immunosuppressive M2 phenotype (Hagemann et al., 2008). In the present study, we report that B cells and FcRg are key parameters regulating pro- versus antitumor programming of macrophages during squamous carcinogenesis through a mechanism that not only involves modified M1 versus M2 or M2-like polarization but also the differential expression of an angiostatic chemokine *Cxcl10* and its receptor *Cxcr3*. As such, activation of angiogenic vasculature in developing tumors is regulated by multiple subsets of myeloid cells, each exhibiting a distinct signature of pro- versus antiangiogenic molecules, as well as likely being programmed by distinct effector pathways dependent on the tissue microenvironment.

These experimental findings imply that reprogramming myeloid cell phenotypes and/or altering the immune microenvironment to foster antitumor versus protumor activity could improve survival of patients with cancer by limiting cancer development and perhaps stabilizing premalignant or premetastatic disease. Proof-of-concept studies supporting this notion were recently reported by De Palma et al. (2008) demonstrating that myeloid cells could be used as vehicles to deliver immune mediators to tumor microenvironments and essentially reprogram them.

Conclusions

Results from this study demonstrate a key role for B lymphocytes, humoral immunity, and activation of FcRg signaling pathways in myeloid cells as promoting forces for squamous carcinogen-esis. With regards to therapy, our data indicate that anti-cancer strategies targeting B cells, Ig, or FcRγ may harbor therapeutic efficacy in limiting risk of malignant conversion in patients suffering from chronic inflammatory diseases or in patients harboring premalignant lesions whose molecular and/or immunologic characteristics favor tumor development. The efficacy and safety of Rituximab for various autoimmune disorders and some hematological cancers could be extended to potentially combat squamous neoplasms in which IC deposition is prominent and/or activation of FcRγ-mediated signaling is evident.

EXPERIMENTAL PROCEDURES

Animal Husbandry

Generation and characterization of HPV16, $JH^{-/-}$, $FcR\gamma^{-/-}$, and $c\text{-}kit^{sh/sh}$ mice have previously been described (Arbeit et al., 1994; Coussens et al., 1996; Lyon and Glenister, 1982; Takai et al., 1994). To generate HPV16 mice in the $JH^{-/-}$ and $FcR\gamma^{-/-}$ backgrounds, $JH^{+/-}$ and $FcR\gamma^{+/-}$ mice were backcrossed into the FVB/n strain to N5 and intercrossed with HPV16 mice. $c\text{-}kit^{sh/+}$ mice were backcrossed five generations into FVB/n. All mouse experiments complied with National Institutes of Health guidelines and were approved by the University of California San Francisco Institutional Animal Care and Use Committee. Characterization of neoplastic stages has been reported previously (Coussens et al., 1996).

In Vivo Assays

For evaluation of proinflammatory properties of IgGs, serum-purified IgGs (20 μl; 12 μg/μl) were injected intradermally into ears of (−)littermates. For performing matrigel plug assays, PDSC5 cells (Arbeit et al., 1996) ($1.5 \times 3\ 10^6$/100 μl) were suspended in 300 ml of Matrigel and injected s.c. in the groin area of 7-week-old mice. For tumorgenicity assays, PDSC5 cells ($0.5 \times 3\ 10^6$ cells) were suspended in 100 ml of Matrigel in PBS (1:1) and inoculated s.c. into flanks of 7-week-old mice. Tumors were measured at 2 day intervals with a digital caliper, and tumor volume was calculated with the equation $V\ (mm^3)=a \times 3\ b^2/2$ (a is the largest diameter and b the smallest diameter).

Low-Density qPCR Arrays

Immune Panel TaqMan arrays (Applied Biosystems) were used to measure the expression of 96 genes in three biological replicates. Analysis of raw data obtained with Immune Panel TaqMan arrays have been performed using an implemented covariance model, as previously described (Pucci et al., 2009).

Statistical Analyses

Statistical analyses were performed using GraphPad Prism version 4 and/or InStat version 3.0a for Macintosh (GraphPad Software). Specific tests included Mann-Whitney (unpaired, nonparametric, two-tailed), unpaired t test, Fisher's exact test, chi-square test, and log rank analysis. p values < 0.05 were considered statistically significant.

Significance

Andreu and colleagues demonstrate that peripheral activation of humoral immunity and subsequent activation of FcγRs on myeloid cells regulate critical features of carcinogenesis that foster solid tumor development. This work reveals previously unrecognized targets for therapeutic intervention in solid tumors, namely, B cells and FcRγ-signaling pathways that work in concert to differentially regulate not only the composition of leukocytes recruited to premalignant tissues but also their bioeffector functions once present.

Supplementary Material

Refer to Web version on PubMed Central for supplementary material.

Acknowledgments

The authors thank the University of California San Francisco Helen Diller Family Comprehensive Cancer Center Laboratory for Cell Analysis and Mouse Pathology shared resource core facilities and members of the Coussens laboratory for critical discussion. The authors acknowledge support from the Cancer Research Institute (P.A.), the Swedish Research Council (M.J.), the American Association for Cancer Research (N.I.A.), the American Cancer Society and National Cancer Institute postdoctoral training grants (T32-CA09043 and T32-CA108462; D.D.), the National Institutes of Health/National Cancer Institute grants (R01CA130980, R01CA13256, R01CA098075, and P01CA72006), and the Department of Defense Breast Cancer Research Program Era of Hope Scholar Award (W81XWH-06-1-0416; L.M.C.). L.N. and M.D.P. were supported by the Associazione Italiana per la Ricerca sul Cancro, the European Union (FP6 Tumor-Host Genomics), and the Italian Ministry of Health (Challenge in Oncology).

REFERENCES

Arbeit JM, Munger K, Howley PM, Hanahan D. Progressive squamous epithelial neoplasia in K14-human papillomavirus type 16 transgenic mice. J. Virol. 1994; 68:4358–4368. [PubMed: 7515971]

Arbeit JM, Olson DC, Hanahan D. Upregulation of fibroblast growth factors and their receptors during multi-stage epidermal carcinogenesis in K14-HPV16 transgenic mice. Oncogene. 1996; 13:1847–1857. [PubMed: 8934530]

Barbera-Guillem E, May KF Jr. Nyhus JK, Nelson MB. Promotion of tumor invasion by cooperation of granulocytes and macrophages activated by anti-tumor antibodies. Neoplasia. 1999; 1:453–460. [PubMed: 10933061]

Barbera-Guillem E, Nelson MB, Barr B, Nyhus JK, May KF Jr. Feng L, Sampsel JW. B lymphocyte pathology in human colorectal cancer. Experimental and clinical therapeutic effects of partial B cell depletion. Cancer Immunol. Immunother. 2000; 48:541–549. [PubMed: 10630306]

Baumann U, Chouchakova N, Gewecke B, Kohl J, Carroll MC, Schmidt RE, Gessner JE. Distinct tissue site-specific requirements of mast cells and complement components C3/C5a receptor in IgG immune complex-induced injury of skin and lung. J. Immunol. 2001; 167:1022–1027. [PubMed: 11441111]

Bergtold A, Gavhane A, D'Agati V, Madaio M, Clynes R. FcR-bearing myeloid cells are responsible for triggering murine lupus nephritis. J. Immunol. 2006; 177:7287–7295. [PubMed: 17082647]

Brandtzaeg P, Carlsen HS, Halstensen TS. The B-cell system in inflammatory bowel disease. Adv. Exp. Med. Biol. 2006; 579:149–167. [PubMed: 16620017]

Chen J, Trounstine M, Alt FW, Young F, Kurahara C, Loring JF, Huszar D. Immunoglobulin gene rearrangement in B cell deficient mice generated by targeted deletion of the JH locus. Int. Immunol. 1993; 5:647–656. [PubMed: 8347558]

Coussens LM, Hanahan D, Arbeit JM. Genetic predisposition and parameters of malignant progression in K14-HPV16 transgenic mice. Am. J. Pathol. 1996; 149:1899–1917. [PubMed: 8952526]

Coussens LM, Raymond WW, Bergers G, Laig-Webster M, Behrendtsen O, Werb Z, Caughey GH, Hanahan D. Inflammatory mast cells up-regulate angiogenesis during squamous epithelial carcinogenesis. Genes Dev. 1999; 13:1382–1397. [PubMed: 10364156]

Coussens LM, Tinkle CL, Hanahan D, Werb Z. MMP-9 supplied by bone marrow-derived cells contributes to skin carcinogenesis. Cell. 2000; 103:481–490. [PubMed: 11081634]

Dalgleish AG, O'Byrne KJ. Chronic immune activation and inflammation in the pathogenesis of AIDS and cancer. Adv. Cancer Res. 2002; 84:231–276. [PubMed: 11883529]

Daniel D, Chiu C, Giraud E, Inoue M, Mizzen LA, Chu NR, Hanahan D. CD4+ T cell-mediated antigen-specific immunotherapy in a mouse model of cervical cancer. Cancer Res. 2005; 65:2018–2025. [PubMed: 15753402]

De Palma M, Mazzieri R, Politi LS, Pucci F, Zonari E, Sitia G, Mazzoleni S, Moi D, Venneri MA, Indraccolo S, et al. Tumortargeted interferon-alpha delivery by Tie2-expressing monocytes inhibits tumor growth and metastasis. Cancer Cell. 2008; 14:299–311. [PubMed: 18835032]

de Visser KE, Korets LV, Coussens LM. Early neoplastic progression is complement independent. Neoplasia. 2004; 6:768–776. [PubMed: 15720803]

de Visser KE, Korets LV, Coussens LM. De novo carcinogenesis promoted by chronic inflammation is B lymphocyte dependent. Cancer Cell. 2005; 7:411–423. [PubMed: 15894262]

de Visser KE, Eichten A, Coussens LM. Paradoxical roles of the immune system during cancer development. Nat. Rev. Cancer. 2006; 6:24–37. [PubMed: 16397525]

DeNardo DG, Baretto JB, Andreu P, Vasquez L, Kolhatkar N, Tawfik D, Coussens LM. CD4+ T cells regulate pulmonary metastasis of mammary carcinomas by enhancing protumor properties of macrophages. Cancer Cell. 2009; 16:91–102. [PubMed: 19647220]

Giraudo E, Inoue M, Hanahan D. An amino-bisphosphonate targets MMP-9-expressing macrophages and angiogenesis to impair cervical carcinogenesis. J. Clin. Invest. 2004; 114:623–633. [PubMed: 15343380]

Gokbuget N, Hoelzer D. Novel antibody-based therapy for acute lymphoblastic leukaemia. Best Pract. Res. Clin. Haematol. 2006; 19:701–713. [PubMed: 16997178]

Gurcan HM, Keskin DB, Stern JN, Nitzberg MA, Shekhani H, Ahmed AR. A review of the current use of rituximab in autoimmune diseases. Int. Immunopharmacol. 2009; 9:10–25. [PubMed: 19000786]

Hagemann T, Lawrence T, McNeish I, Charles KA, Kulbe H, Thompson RG, Robinson SC, Balkwill FR. “Re-educating” tumor-associated macrophages by targeting NF-kappaB. J. Exp. Med. 2008; 205:1261–1268. [PubMed: 18490490]

Junankar SR, Eichten A, Kramer A, de Visser KE, Coussens LM. Analysis of immune cell infiltrates during squamous carcinoma development. J. Investig. Dermatol. Symp. Proc. 2006; 11:36–43.

Lu H, Goodell V, Disis ML. Humoral immunity directed against tumor-associated antigens as potential biomarkers for the early diagnosis of cancer. J. Proteome Res. 2008; 7:1388–1394. [PubMed: 18311901]

Lyon MF, Glenister PH. A new allele sash (Wsh) at the W-locus and a spontaneous recessive lethal in mice. Genet. Res. 1982; 39:315–322. [PubMed: 7117838]

Mantovani A, Allavena P, Sica A, Balkwill F. Cancer-related inflammation. Nature. 2008; 454:436–444. [PubMed: 18650914]

Markiewski MM, DeAngelis RA, Benencia F, Ricklin-Lichtsteiner SK, Koutoulaki A, Gerard C, Coukos G, Lambris JD. Modulation of the antitumor immune response by complement. Nat. Immunol. 2008; 9:1225–1235. [PubMed: 18820683]

Nakayama T, Yao L, Tosato G. Mast cell-derived angiopoietin-1 plays a critical role in the growth of plasma cell tumors. J. Clin. Invest. 2004; 114:1317–1325. [PubMed: 15520864]

Nimmerjahn F, Ravetch JV. Fcgamma receptors as regulators of immune responses. Nat. Rev. Immunol. 2008; 8:34–47. [PubMed: 18064051]

Ostrand-Rosenberg S. Immune surveillance: a balance between protumor and antitumor immunity. Curr. Opin. Genet. Dev. 2008; 18:11–18. [PubMed: 18308558]

Pollard JW. Macrophages define the invasive microenvironment in breast cancer. J. Leukoc. Biol. 2008; 84:623–630. [PubMed: 18467655]

Pucci F, Venneri MA, Biziato D, Nonis A, Moi D, Sica A, Di Serio C, Naldini L, De Palma M. A distinguishing gene signature shared by tumor-infiltrating Tie2-expressing monocytes (TEMs), blood “resident” monocytes and embryonic macrophages suggests common functions and developmental relationships. Blood. 2009; 114:901–914. [PubMed: 19383967]

Shah S, Divekar AA, Hilchey SP, Cho HM, Newman CL, Shin SU, Nechustan H, Challita-Eid PM, Segal BM, Yi KH, Rosenblatt JD. Increased rejection of primary tumors in mice lacking B cells: inhibition of anti-tumor CTL and TH1 cytokine responses by B cells. Int. J. Cancer. 2005; 117:574–586. [PubMed: 15912532]

Siegel CT, Schreiber K, Meredith SC, Beck-Engeser GB, Lancki DW, Lazarski CA, Fu YX, Rowley DA, Schreiber H. Enhanced growth of primary tumors in cancer-prone mice after immunization against the mutant region of an inherited oncoprotein. J. Exp. Med. 2000; 191:1945–1956. [PubMed: 10839809]

Soucek L, Lawlor ER, Soto D, Shchors K, Swigart LB, Evan GI. Mast cells are required for angiogenesis and macroscopic expansion of Myc-induced pancreatic islet tumors. Nat. Med. 2007; 13:1211–1218. [PubMed: 17906636]

Takai T. Fc receptors and their role in immune regulation and autoimmunity. J. Clin. Immunol. 2005; 25:1–18. [PubMed: 15742153]

Takai T, Li M, Sylvestre D, Clynes R, Ravetch JV. FcR gamma chain deletion results in pleiotrophic effector cell defects. Cell. 1994; 76:519–529. [PubMed: 8313472]

Tan TT, Coussens LM. Humoral immunity, inflammation and cancer. Curr. Opin. Immunol. 2007; 19:209–216. [PubMed: 17276050]

Theoharides TC, Conti P. Mast cells: the Jekyll and Hyde of tumor growth. Trends Immunol. 2004; 25:235–241. [PubMed: 15099563]

Zapata JM, Llobet D, Krajewska M, Lefebvre S, Kress CL, Reed JC. Lymphocyte-specific TRAF3 transgenic mice have enhanced humoral responses and develop plasmacytosis, autoimmunity, inflammation, and cancer. Blood. 2009; 113:4595–4603. [PubMed: 19074733]

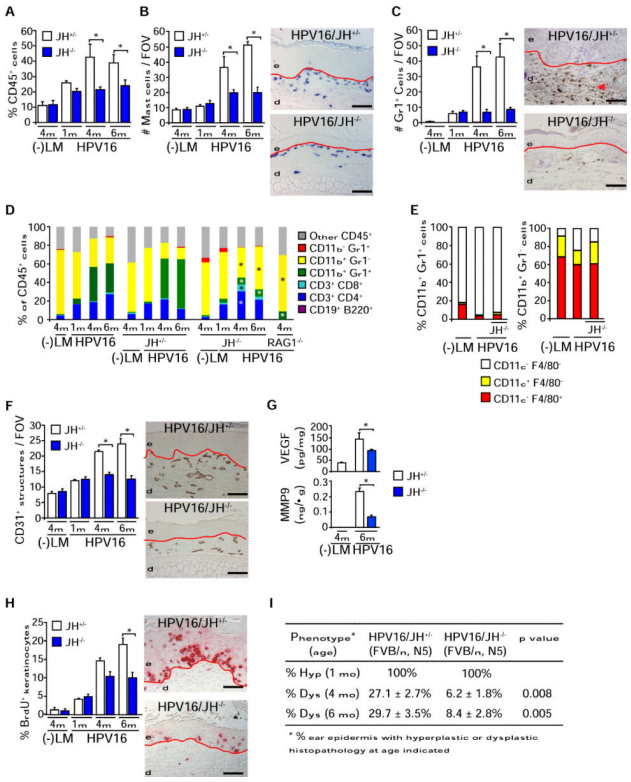

Figure 1. B Cells Are Critical Regulators of Premalignant Progression in HPV16 Mice

(A) Percentage of $CD45^+$ cells in skin single cell suspensions isolated from negative littermates (−LM), HPV16/$JH^{+/-}$, and HPV16/$JH^{-/-}$ mice at 1, 4, and 6 months of age assessed by flow cytometry.

(B and C) Mast cells (B, blue staining) and $Gr1^+$ myeloid cells (C, brown staining) in skin of HPV16/$JH^{+/-}$ and HPV16/$JH^{-/-}$ mice at 1, 4, and 6 months of age assessed quantitatively after chloroacetate esterase histochemistry or Gr1 immunohistochemistry (IHC), respectively.

(D) Flow cytometric analysis of immune cell lineages expressed as percentages of total $CD45^+$ leukocyte infiltrates in ear tissue of negative littermates (−LM), HPV16, HPV16/$JH^{+/-}$, HPV16/$JH^{-/-}$, and HPV16/$RAG1^{-/-}$ mice at 1, 4, and 6 months of age.

(E) Dendritic ($CD11c^+$) and macrophage ($F4/80^+$) lineage cell composition of $CD11b^+Gr1^+$ (left) and $CD11b^+Gr1^-$ (right) myeloid populations evaluated by flow cytometry in skin of negative littermates (−LM), HPV16, and HPV16/$JH^{-/-}$ mice at 4 months of age.

(F) Angiogenic vasculature in skin tissue sections from negative littermates (−LM), HPV16/$JH^{+/-}$, and HPV16/$JH^{-/-}$ mice at 1, 4, and 6 months of evaluation by CD31/PECAM-1 IHC revealing endothelial cells (brown staining).

(G) Reduced VEGF-A and active MMP-9 protein levels in skin extracts from HPV16/$JH^{-/-}$ versus HPV16/$JH^{+/-}$ mice (4 and 6 months) as assessed by ELISA.

(H) Keratinocyte proliferation in skin of negative littermates (−LM), HPV16/$JH^{+/-}$, and HPV16/$JH^{-/-}$ mice at 1, 4, and 6 months of age, as evaluated by quantitation of bromodeoxyuridine (BrdU)-positive keratinocytes (red staining).

(I) Percentage of ear skin in HPV16/$JH^{-/-}$ and HPV16/$JH^{+/-}$ mice developing hyperplastic lesions by 1 month of age (Hyp) or dysplasia by 4 and 6 months of age (Dys).

(A–I) Results shown represent mean ± SEM (n = 5–8 mice) and asterisks (*) indicate statistically significant differences ($p < 0.05$, Mann-Whitney). Representative images of HPV16/$JH^{+/-}$ and HPV16/$JH^{-/-}$ mouse skin at 4 months of age are shown. Values represent

average of five high-power fields of view per mouse and five mice per category. FOV, field of view; solid red line, epidermal-dermal interface; e, epidermis; d, dermis. Scale bars represent 50 μm. See also Figure S1.

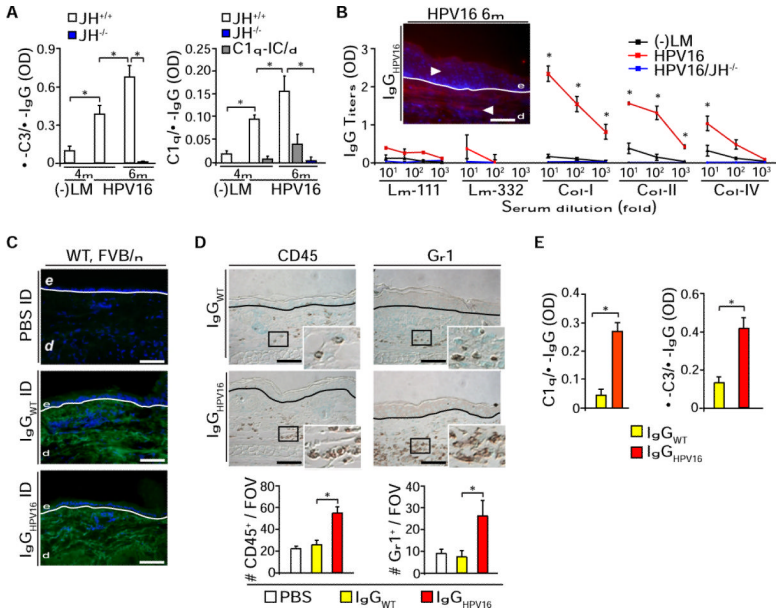

Figure 2. CICs from HPV16 Mice Induce Acute Inflammation

(A) CICs titers in serum collected from negative littermate (−LM), HPV16/JH$^{+/+}$, and HPV16/JH$^{-/-}$ mice assessed by ELISA with anti-mouse C3 Ig (left) and C1q (right). The specificity of C1q/IgG binding to ICs was assessed by disrupting C1q-CIC binding using a high-salt solution (C1q/IC/d; gray bars).

(B) Antibody titers for laminin (Lm)-111, Lm-332, collagen (Col)-I, Col-II, and Col-IV in serum from littermate (−LM), HPV16, and HPV16/JH$^{-/-}$ (4 months) were evaluated by indirect ELISA. Antigens recognized by biotinylated IgG$_{HPV16}$ were localized by immunofluorescence on skin sections from 4-month-old HPV16 mice (inset; IgGs: red staining).

(C) Immunofluorescence (green staining) staining on syngeneic skin tissue sections reveals presence of intradermally injected purified IgGs isolated from negative littermate (IgG$_{wt}$) or HPV16 (IgG$_{HPV16}$) 24 hr after intradermal injections.

(D) Number of infiltrating CD45^{+} leukocytes and Gr1^{+} cells in skin tissue sections 24 hr after intradermal injections of PBS, IgG$_{wt}$, or IgG$_{HPV16}$ into ears of syngeneic wild-type FVB/n mice. Values reflect averages from five high-power fields per mouse.

(E) Normalized CIC titers of IgG purified from negative littermates (IgG$_{wt}$) or HPV16 (IgG$_{HPV16}$) serum assessed by ELISA with anti-mouse C3 Ig (left) and C1q (right).

(B and C) Blue staining, DAPI; white line, epidermal-dermal interface; e, epidermis; d, dermis. Scale bars represent 50 μm.

(B–D) Results shown are mean percentages ± SEM (n = 5–8 mice) and asterisks (*) indicate statistically significant differences ($p < 0.05$, Mann-Whitney). See also Figure S2.

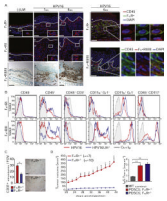

Figure 3. Infiltration of FcγR$^+$ Leukocytes during Neoplastic Progression in HPV16 Mice

(A) Infiltration of leukocytes expressing FcRγ (red staining, top), FcγRI (red staining, middle), and FcγRII/III (brown staining, bottom) in premalignant skin of HPV16 mice evaluated in tissue sections by immunofluorescence. Shown in the right panels is double immunofluorescence staining revealing expression of FcRγ and FcγRII/III on CD45$^+$ leukocytes. Solid line, epidermal-dermal interface; e, epidermis; d, dermis; blue staining, DAPI. Scale bars represent 50 μm.

(B) Differential expression of FcγRI and FcγRIII by individual leukocyte populations in premalignant skin of HPV16 (red) and HPV16/JH$^{-/-}$ (blue) mice at 4 months of age. Live cells were gated as CD45$^+$ leukocytes, CD45$^+$CD3$^+$ T lymphocytes, CD11b$^+$Gr1$^+$ IMCs, CD11b$^+$Gr1$^-$ mixed macrophages/DCs, and CD45$^+$CD117$^+$ mast cells. Grey line, Ig control.

(C) PDSC5 tumor cells were injected as matrigel plugs into FcRγ$^{+/-}$ and FcRγ$^{-/-}$ mice (FVB/n). Neovascularization was evaluated by CD31 IHC (brown staining). Values reflect number of CD31$^+$ vessels averaged from five high-power fields per mouse (n = 5–8 mice). Scale bars represent 25 μm.

(D) Deficient tumor growth in mice lacking FcRγ. PDSC5 tumor cells were injected s.c. into FcRγ$^{+/-}$ and FcRγ$^{-/-}$ syngeneic FVB/n mice. Titers of IgG in serum of wild-type (WT) FVB/n versus transplanted FVB/n mice evaluated by ELISA.

(C and D) Results shown are mean percentages ± SEM. Asterisks (*) indicate statistically significant differences ($p < 0.05$, unpaired t test).

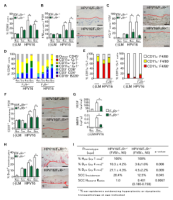

Figure 4. FcRγ Expression Is a Critical Determinant of Squamous Carcinogenesis in HPV16 Mice

(A) Percentage of $CD45^+$ cells in skin of HPV16/$FcR\gamma^{+/-}$ and HPV16/$FcR\gamma^{-/-}$ mice at 1, 4, and 6 months assessed by flow cytometry.

(B and C) Mast cells (B, blue staining) and $Gr1^+$ myeloid cells (C, brown staining) in skin of HPV16/$FcR\gamma^{+/-}$ and HPV16/$FcR\gamma^{-/-}$ mice at 1, 4, and 6 months of age assessed quantitatively after chloroacetate esterase histochemistry or Gr1 IHC, respectively.

(D) Flow cytometric analysis of immune cell lineages as percentages of total $CD45^+$ leukocytes in single-cell suspensions from nontransgenic, HPV16/$FcR\gamma^{+/-}$, and HPV16/$FcR\gamma^{-/-}$ transgenic skin at 1, 4, and 6 months of age.

(E) Dendritic ($CD11c^+$) and macrophage ($F4/80^+$) cell composition in $CD11b^+Gr1^+$ and $CD11b^+Gr1^-$ myeloid populations evaluated by flow cytometry of single cell suspensions derived from skin of negative littermate (−LM), HPV16, and HPV16/$FcR\gamma^{-/-}$ mice at 4 months of age.

(F) Attenuated angiogenesis in premalignant skin of HPV16/$FcR\gamma^{-/-}$ mice. Density of angiogenic vasculature evaluated quantitatively by CD31 IHC (brown staining) on age-matched tissue sections.

(G) Reduction in total VEGF-A and active MMP-9 protein levels in skin tissue extracts from age-matched HPV16/$FcR\gamma^{-/-}$ and HPV16/$FcR\gamma^{+/-}$ mice as determined by ELISA.

(H) Keratinocyte proliferation evaluated as percentage of bromodeoxyuridine (BrdU)-positive keratinocytes (red staining) in ear skin tissue sections representing age-matched negative littermate (−LM), HPV16/$FcR\gamma^{+/-}$, and HPV16/$FcR\gamma^{-/-}$ premalignant skin.

(I) Percentages of ear skin (area) exhibiting hyperplasia by 1 month of age (Hyp) or dysplasia by 4 or 6 months of age (Dys). Values represent percentages of mice with specific neoplastic phenotypes. Statistical significance was determined using the Mann-Whitney test. Lifetime incidence of SCC was determined in HPV16/$FcR\gamma^{+/-}$ and HPV16/$FcR\gamma^{-/-}$ mice (97 and 132 mice/group, respectively). Tumor incidence was analyzed with the generalized Wilcoxon test. Hazard ratio was determined by Kaplan Meyer analysis of tumor incidence. All mice reflect similarly backcrossed groups at FVB/n, N5.

(A–H) Results shown represent mean ± SEM (n = 5–8 mice) and asterisks (*) indicate statistically significant differences ($p < 0.05$, Mann-Whitney). Values represent average of five high-power fields of view per mouse. Representative images of HPV16/$FcR\gamma^{+/-}$ and HPV16/$FcR\gamma^{-/-}$ skin tissue sections at 4 months of age are shown. Red line, epidermal-dermal interface; e, epidermis; d, dermis. Scale bars represent 50 μm. See also Figure S3.

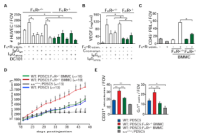

Figure 5. Activating FcγRs Regulate Protumor Functions of Mast Cells

(A) FcγR-dependent chemotaxis of HUVECs in response to FcγR-stimulated mast cells isolated from FcRγ$^{+/-}$ or FcRγ$^{-/-}$ mice. BMMCs were stimulated with 2.4G2 and anti-rat IgG (25 μg/ml; FcγR-stim.), IgG_{HPV16}, or IgG_{wt} (30 μg/ml). HUVEC migration in response to conditioned medium was assessed using a Boyden chamber assay. A specific VEGF-R2 inhibitor (DC101; 100 μg/ml) was used. HUVEC migration was quantitated by enumerating the number of migrating cells in four random fields per membrane (125× magnification). Samples were assayed in quadruplet for each assessed condition.

(B) BMMCs from FcRγ$^{+/-}$ or FcRγ$^{-/-}$ mice were FcγR stimulated or activated with IgG_{HPV16} or IgG_{wt} in the presence or absence of the mast cell stabilizer cromolyn (10 μM). Levels of VEGF-A in conditioned medium were assessed by ELISA. Representative analysis from three independent experiments is shown.

(C) PBL migration in response to conditioned medium from FcRγ$^{+/-}$ versus FcRγ$^{-/-}$ BMMCs after FcγR stimulation was evaluated with a Boyden chamber assay. PBLs migrating to the lower chamber were visualized by H&E staining in five to eight random fields per well. Samples were assayed in triplicate for each tested condition.

(D) FcRγ-proficient mast cells enhance tumorigenicity. PDSC5 tumor cells (blue) alone or admixed with FcRγ$^{+/-}$ (red) or FcRγ$^{-/-}$ (green) BMMCs were injected s.c. into FVB/n (WT) or kit$^{sh/sh}$ (gray) mice at a 1:1 ratio. The asterisk (*) indicates statistically significant differences between PDSC5 cells in combination with FcRγ$^{+/-}$ versus FcRγ$^{-/-}$ BMMCs. The number sign (#) indicates statistically significant differences between tumor growth in syngeneic FVB/n or kit$^{sh/sh}$ mice.

(E) FcRγ-proficient mast cells induce angiogenesis and leukocyte infiltration of transplantable tumors. Blood vessels and leukocyte infiltration were evaluated by CD31 and Gr1 IHC. Values represent average of five high-power fields of view per tumor and six to ten tumors per category.

(A–E) Data are represented as means ± SEM; *$p < 0.05$; **$p < 0.01$ (unpaired t test).

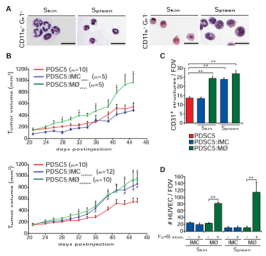

Figure 6. Tumor-Promoting Activities of CD11b^{+}Gr1$^{+/-}$ Myeloid Cells in HPV16 Mice

(A) Representative micrographs depicting morphology of CD11b^{+}Gr1^{+} and CD11b^{+}Gr1^{-} myeloid cells purified by FACS sorting from skin or spleen of HPV16 mice (4 month) and visualized via May-Grünwald-Giemsa staining (scale bars represent 50 μm).

(B) Macrophages and spleen IMCs enhance tumorgenicity. Tumor growth of PDSC5 cells alone (red line) or admixed with either IMCs (blue line) or macrophages (MØ, green line; PDSC5/leukocyte = 10:1) FACS sorted from neoplastic skin (top graph) or spleen (bottom graph) of HPV16 mice at 4 months of age. Asterisks (*) and number signs (#) indicate statistically significant differences between PDSC5 cells alone and PDSC5 in combination with macrophages and IMCs, respectively.

(C) Macrophages and spleen IMCs enhance tumor angiogenesis. Blood vessels in PDSC5 subcutaneous tumors were evaluated by CD31 and Gr1 IHC. Values represent average of five high-power fields of view per tumor and six to ten tumors per category.

(D) FcγR-stimulated macrophages are chemotactic toward endothelial cells. Macrophages and IMCs were purified by FACS sorting from neoplastic skin and spleens of 4-month-old HPV16 mice and treated for IgG-dependent FcγR stimulation and HUVEC chemotaxis was evaluated in a Boyden chamber assay.

(B–D) Data are represented as means ± SEM (*, $^{\#}p < 0.01$; **$p < 0.001$, unpaired t test). See also Figure S4 and Table S1.

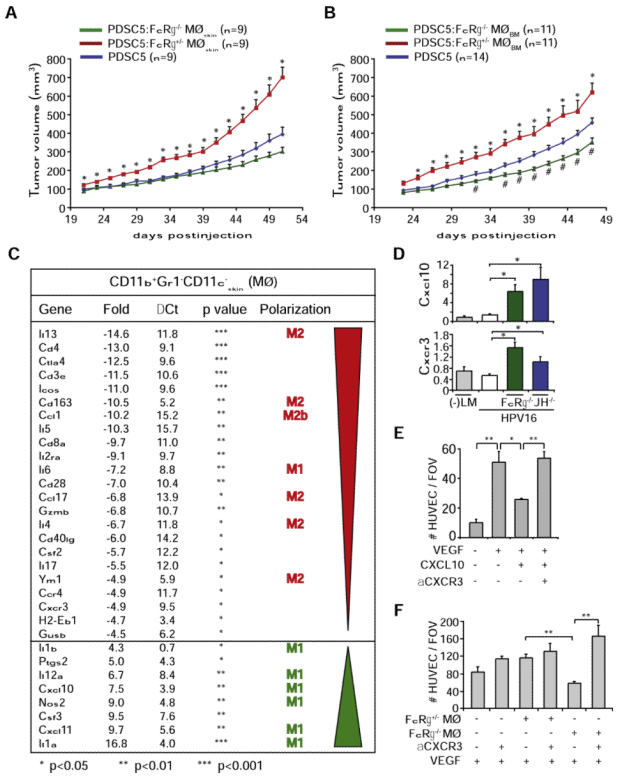

Figure 7. FcRγ Expression Regulates Proangiogenic and Protumorigenic Properties of Macrophages

(A and B) FcRγ expression regulated macrophage protumor activity. PDSC5 tumor cells were injected alone (blue) or admixed with macrophages derived from neoplastic skin ($MØ_{skin}$) of either HPV16/FcRγ$^{+/-}$ (red) or HPV16/FcRγ$^{-/-}$ (green) mice (A) or instead from bone marrow-derived macrophages ($MØ_{BM}$) isolated from FcRγ$^{+/-}$ (red) or FcRγ$^{-/-}$ (green) mice (B). The asterisk (*) indicates statistically significant differences between PDSC5 cells admixed with FcRγ$^{+/-}$ versus FcRγ$^{-/-}$ macrophages. The number sign (#) indicates statistically significant differences between PDSC5 alone and PDSC5 admixed with FcRγ$^{-/-}$ macrophages. Data are represented as means ± SEM; $p < 0.05$, unpaired t test.

(C) Genes differentially expressed in macrophages isolated from neoplastic skin of HPV16/FcRγ$^{-/-}$ versus HPV16/FcRγ$^{+/-}$ mice. mRNA expression levels in macrophages from HPV16/FcRγ$^{-/-}$ neoplastic skin (4 month old) are indicated as fold change as compared to HPV16/FcRγ$^{+/-}$ macrophages with ΔCT of each gene calculated with *β2-microglobulin* as endogenous control. Expression was considered as statistically significantly deregulated when $p < 0.05$ (t test, FcRγ$^{-/-}$ versus FcRγ$^{+/-}$).

(D) Quantitative real-time PCR analysis of *Cxcl10* and *Cxcr3* mRNA expression in ear tissue from 4-month-old negative littermate (−LM), HPV16, HPV16/JH$^{-/-}$, and HPV16/FcRγ$^{-/-}$ mice (n = 3–5 mice/cohort). *$p < 0.05$; **$p < 0.01$, unpaired t test.

(E) $VEGF_{165}$-induced (100 ng/ml) HUVEC chemotaxis was evaluated in a Boyden chamber assay after pretreatment with recombinant CXCL10 (100 ng/ml) in the presence or absence of CXCR3 blocking antibody (10 μg/ml). *$p < 0.05$; **$p < 0.01$, unpaired t test.

(F) Macrophages isolated from HPV16/FcRγ$^{-/-}$ mice exhibit angiostatic activity. HUVEC chemotaxis in a Boyden chamber assay was evaluated after pretreatment with conditioned medium isolated from macrophages (purified from skin of HPV16/FcRγ$^{+/-}$ or HPV16/FcRγ$^{-/-}$ mice) following activation with LPS (10 ng/ml) and αCXCR3 blocking Ig (10 μg/ml). *, $p < 0.05$; **, $p < 0.01$, unpaired t test.

(E and F) Pretreated HUVECs were evaluated for chemotactic migration in response to VEGF (100 ng/ml) using a Boyden chamber assay. Quantitative values reflect the number of migrating HUVECs averaged from four to five high-power fields per insert and four inserts per treatment ± SEM. At least three independent analyses were performed and one representative experiment is shown. See also Figure S5 and Table S1.

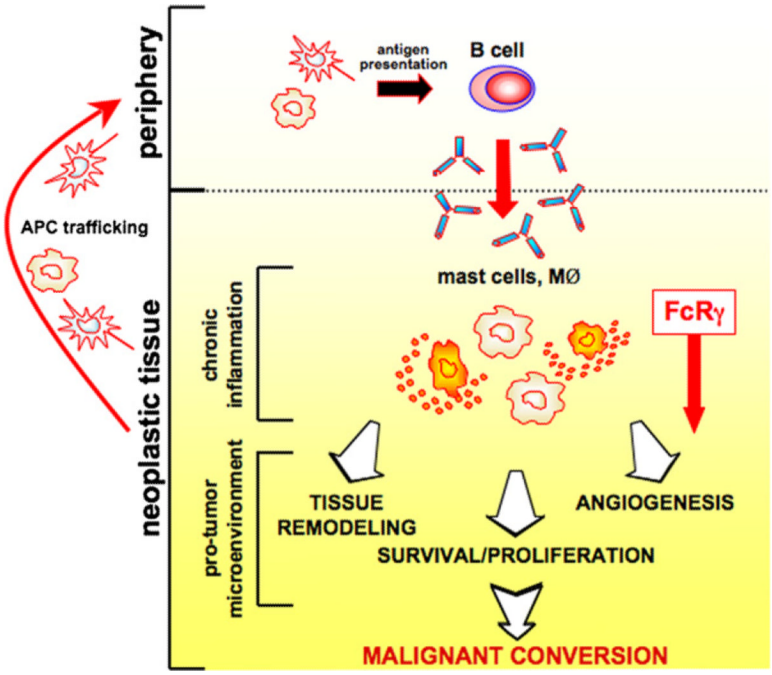

Figure 8. Activation of the FcRγ Pathway in Mast Cells and Macrophages by Humoral Immunity Regulates Squamous Carcinogenesis of HPV16 Mice

HPV16 oncogene expression initiates keratinocytes and triggers early neoplastic progression accompanied by neo- and self-antigen presentation, peripheral B cell activation/maturation, and secretion of Igs. Autoantibodies subsequently accumulate in dermal stroma of neoplastic tissue as vasculature becomes initially angiogenic and “leaky.” IgGs interact with Fcγ receptors on resident and recruited myeloid cells where they induce differential recruitment of leukocytes from peripheral blood and regulate mast cell and macrophage bioeffector functions once present in neoplastic tissue. FcRγ deficiency not only impairs the protumorigenic properties of mast cells and macrophages but also reprogram macrophages leading to enhanced angiostatic and M1 bioactivity.